Influence of Magnetic Field Strength and Image Registration Strategy on Voxel-based Morphometry in a Study of Alzheimer's Disease

Artur Marchewka,[1,2]* Ferath Kherif,[1] Gunnar Krueger,[3] Anna Grabowska,[4] Richard Frackowiak,[1] Bogdan Draganski[1,5] and The Alzheimer's Disease Neuroimaging Initiative

[1]*LREN, Département des Neurosciences Cliniques, CHUV, University of Lausanne, Lausanne, Switzerland*
[2]*Laboratory of Brain Imaging, Neurobiology Centre, Nencki Institute of Experimental Biology, Warsaw, Poland*
[3]*Healthcare Sector IM&WS S, Siemens Schweiz AG, Renens, VD, Switzerland*
[4]*Laboratory of Psychophysiology, Department of Neurophysiology, Nencki Institute of Experimental Biology, Warsaw, Poland*
[5]*Max-Planck Institute for Human Cognitive and Brain Sciences, Leipzig, Germany*

Abstract: Multi-centre data repositories like the Alzheimer's Disease Neuroimaging Initiative (ADNI) offer a unique research platform, but pose questions concerning comparability of results when using a range of imaging protocols and data processing algorithms. The variability is mainly due to the non-quantitative character of the widely used structural T1-weighted magnetic resonance (MR) images. Although the stability of the main effect of Alzheimer's disease (AD) on brain structure across platforms and field strength has been addressed in previous studies using multi-site MR images, there are only sparse empirically-based recommendations for processing and analysis of pooled multi-centre structural MR data acquired at different magnetic field strengths (MFS). Aiming to minimise potential systematic bias when using ADNI data we investigate the specific contributions of spatial registration strategies and the impact of MFS on voxel-based morphometry in AD. We perform a whole-brain analysis within the framework of Statistical Parametric Mapping, testing for main effects of various diffeomorphic spatial registration strategies, of MFS and their interaction with disease status. Beyond the confirmation of medial temporal lobe volume loss in AD, we detect a significant impact of spatial registration strategy on estimation of AD related atrophy. Additionally, we report a significant effect of MFS on the assessment of brain anatomy (i) in the cerebellum, (ii) the precentral gyrus and (iii) the thalamus bilaterally, showing no interaction with the disease status. We provide empirical evidence in support of pooling data in multi-centre VBM studies irrespective of disease status or MFS. *Hum Brain Mapp 00:000–000, 2013.*

Key words: voxel-based morphometry; multi-centre study; diffeomorphic registration; disease-specific template

*Correspondence to: Artur Marchewka, Département des neurosciences cliniques - CHUV, University Lausanne, Rue du Bugnon 46, 1011 Lausanne, Switzerland.
E-mail: a.marchewka@nencki.gov.pl

Received for publication 2 April 2012; Revised 23 January 2013; Accepted 6 March 2013
DOI: 10.1002/hbm.22297
Published online in Wiley Online Library (wileyonlinelibrary.com).

INTRODUCTION

The steadily growing popularity and utilisation of multi-centre brain imaging data for voxel-based morphometry (VBM) in neurodegeneration is challenged by the scarcity of empirical data looking for a potentially significant impact of magnetic field strength (MFS), radio-frequency (RF) transmit bias, and data processing strategy on the obtained results (Focke et al., 2011). The VBM algorithms are typically applied to non-quantitative T1-weighted (T1w) high-resolution structural magnetic resonance (MR) images, where automated tissue classification and spatial registration to standardized stereotactic space is followed by a voxel-based statistical analysis to identify regional volume differences within or between cohort(s). Importantly, brain atrophy measures based on T1w images are shown to correlate with the amount of tau deposition and neuropsychological deficits, thus validating its use as a biomarker of Alzheimer's disease (AD) (Frisoni et al., 2010).

Current projects involving MR imaging data repositories, such as the Biomedical Informatics Research Network (www.birncommunity.org), the AddNeuroMed (www.innomed-addneuromed.com) or the Alzheimer's Disease Neuroimaging Initiative (ADNI) provide opportunities to study large numbers of subjects, resulting in increased sensitivity for the detection of subtle disease related effects. On the other hand, pooling data from different MR scanner and MFSs could introduce systematic errors. Therefore, from the user's perspective it is crucial to be aware of potential limitations of the VBM analysis when using large data sets under these circumstances. Stonnington et al. (2008) compared ADNI data collected at 1.5 Tesla (T) MFS to demonstrate convincingly that scanner-associated differences are substantially less than those related to diagnosis and also that there is no interaction between the two. A significant scanner related effect was observed only in the thalamus (see also Raz et al., 2005).

Much less is known about the effects of MFS (1.5T vs. 3T) on morphometric analyses of neurodegeneration using T1w anatomical images. Previous volumetric region-of-interest studies on hippocampus and amygdala failed to demonstrate a specific impact of MFS on volumetric assessments of these structures in patients with epilepsy (Briellmann et al., 2001; Scorzin et al., 2008). Similarly, cortical thickness estimation and correlations with cognitive performance have proved reliable at different MFSs (Dickerson et al., 2008; Han et al., 2006). Recent studies performed at 1.5T and 3T reported an agreement between the volume estimates of age/disease dependent changes at both field strengths (Goodro et al., 2012; Pfefferbaum et al., 2012). On the contrary, there are studies reporting interaction between acquisition protocols [e.g. fast low-angle shot, magnetization-prepared rapid gradient-echo (MP-RAGE)] and MFS resulting in differential voxel-based volume estimation of cortical and sub-cortical structures at different field strength (Pardoe et al., 2008; Tardif et al., 2010).

To the best of our knowledge the effect of MFS on VBM analysis of T1w images has never been directly evaluated on a large multi-site data set in neurodegenerative disorders. The first aim of our study was to investigate the impact of MFS (1.5 and 3 T) and effect of diagnosis on well-established AD-related structural brain changes to justify pooling images collected in a multi-centre setting. From an anatomical perspective we sought to explore the specific effect of MFS on VBM results in neurodegeneration. Considering findings from previous studies (Dickerson et al., 2008; Han et al., 2006; Stonnington et al., 2008) we hypothesize the presence of specific regional effects of MFS in cortical and subcortical regions and an interaction between MFS and disease-related volume changes.

Image registration is another potentially important confound at the stage of pooling multi-scanner data sets. Until recently much effort has been put into increasing the accuracy and reliability of spatial registration algorithms to a common reference template. Algorithms such as Diffeomorphic Anatomical Registration Through Exponentiated Lie Algebra (DARTEL) have been proposed to improve inter-subject registration (Ashburner, 2007) by generating a customised, study-specific spatial template that represents the characteristics of the sample (e.g. scanner-specific or disease-specific). Comparative studies using Statistical Parametric Mapping (SPM) have confirmed that the diffeomorphic alignment to study-specific templates provides better spatial registration than previous standard SPM registration procedures in both AD patients and cognitively normal elderly adults [Klein et al., 2009 (see for algorithms comparison); Pereira et al., 2010; Takahashia et al., 2010]. Considering previous controversies about the impact of population selection on the robustness and bias introduced by tissue-specific spatial template (Lepore et al., 2008), the second objective of this study is to investigate the effect of disease-specific spatial templates on multi-centre data VBM results. We decide for an empirical approach because of the potential upside of being able to reliably pool data from different sources for multi-centre studies, studies of rare and orphan diseases and for ease of cohort construction.

In an effort to determine the influences of both MFS and image registration strategy on disease-related volume changes we use images from the ADNI database and SPM8 software. Given there is no quantitative method for comparing VBM pre-processing algorithms besides comparison to empirically derived information we report a qualitative comparison of our findings with well-established anatomical distribution patterns associated with AD pathology (Braak and Braak, 1991; Frisoni et al., 2010; Hyman et al., 1997).

MATERIAL AND METHODS

Subjects and Data Acquisition

For our study we use MR data from the ADNI database acquired at a single time-point at 28 different centres

TABLE I. Subjects' demographic summary

Group	Subjects (F/M)	MFS	MMSE (range)	Age (range)
Patients	42 (21/22)	1.5 T	23.3 (20–26)	77.6 (63–88)
	17 (10/7)	3 T	22.4 (20–26)	76.1 (63–91)
Controls	54 (27/27)	1.5 T	29.2 (26–30)	76.9 (62–88)
	27 (19/8)	3 T	29.3 (26–30)	75 (60–87)

MFS, Magnetic field strength; MMSE, Mini-Mental State Exam; F, Female; M, Male.

(Mueller et al., 2005). We include AD patients ($n = 59$) with different degree of memory impairment assessed with the Mini-Mental State Exam (MMSE) score and healthy controls ($n = 81$) (for demographic and clinical summary see Table I). Subjects were scanned on four different Siemens scanner platforms operating at two different MFSs (1.5T Avanto, 1.5T Symphony, 3T Allegra, 3T Trio) and using a multi-channel phased-array head-coil. According to the ADNI protocol the T1w data was acquired according to a standardised MP-RAGE protocol (see Table II and www.adni.loni.ucla.edu/research/protocols/mri-protocols) followed by correction for gradient non-linearity and intensity non-uniformity (Jack et al., 2008).

Processing of Structural Data

Data pre-processing and analysis is performed with the freely available SPM8 software (Wellcome Trust Centre for Neuroimaging, London, UK) running under MATLAB 7.10 (Mathworks, Sherborn, MA). T1w scans are automatically classified into grey matter, white matter and cerebrospinal fluid using the "New Segmentation" tool based on a mixture of Gaussian models and tissue probability maps (Ashburner and Friston, 2005).

In a subsequent step we apply the default settings of the diffeomorphic registration algorithm DARTEL (Ashburner, 2007). For this step we assign six different combinations (further referred to as pre-processing ROUTINES) of registration according to diagnosis, MFS and gender (see Table II). For each ROUTINE we use the same data set. In ROUTINE 1 all subjects are pooled together for diffeomorphic registration resulting in one common study-specific template. In ROUTINE 2 registration is based on separate cohorts defined by disease status (patients vs. controls) irrespective of scanner MFS; consequently we create patient and control subject-specific templates. In ROUTINE 3 the diffeomorphic registration is based on cohorts defined by the MFS—1.5T and 3T resulting in two field strength specific templates. For ROUTINE 4 the diffeomorphic registration is performed on cohorts defined by group and by MFS, which results in four group by MFS templates. In ROUTINE 5 the registration is based on cohorts defined by random assignment of the whole data set into two subgroups. Finally, for ROUTINE 6 registration we create a "balanced template" based on equal numbers of images from each of the eight studied subgroups defined by disease status, MFS and gender—there were in total 56 images, seven for each of the studied subgroups (for ROUTINES summary see Table III).

At the final stage, images in each of the pre-processing strategies are affine registered to the standard Montreal Neurological Institute – MNI space (Ashburner, 2007), followed by scaling the GM probability values with the Jacobian determinants to ensure preservation of the total signal in each tissue class (i.e. "modulation") (Ashburner and Friston, 2000). Finally, the volume maps are smoothed with a 6-mm full-width-at-half-maximum Gaussian kernel. Total intracranial volume is calculated for each individual by summing together the voxel values of the grey matter, white matter and CSF (for details see the existing recommendations on VBM data pre-processing under SPM - www.fil.ion.ucl.ac.uk/~john/misc/VBMclass10.pdf).

STATISTICAL ANALYSIS

Demographic and Clinical Data Analysis

For the analysis of demographic and clinical data we use an analysis of variance (ANOVA) model with two factors - GROUP (two levels—AD patients and healthy subjects) and MFS (two levels—1.5T and 3T) under SPSS 17.0 (http://www.spss.com/statistics/). The adjustment for multiple comparisons is performed using Bonferroni correction.

Voxel-based Morphometry Analysis

For computation of main effects and interaction between MFS and data pre-processing strategy on the differentiation between AD patients and control subjects we use a full-factorial analysis. For each data pre-processing ROUTINE we assign the factor GROUP with two levels indicating the most probable diagnosis based on clinical features and the MMSE score - AD or healthy controls (CR); and

TABLE II. Range of typically selected parameters for MP-RAGE acquisition in the studied sample. TR is defined here as the repetition time for the inversion pulses

Bo	No. of slices	FoV (mm)	TR (ms)	T1 (ms)	Flip	Plane
1.5T	160–170	240 × 240	2300–2400	1000	8	Sagittal PE
3T	160–170	256–260 × 240	2300 or 3000	853–900	8–9	Sagittal PE

TABLE III. Routine (ROU) indicates type of pre-processing, routine 1—all subjects pooled together for registration; routine 2 registration within separate cohorts defined by factor GROUP (patients vs. controls) irrespective of MFS or scanner type; routine 3—registration within separate cohorts defined by factor MFS (1.5T patients & controls, 3T patients & controls); routine 4—registration within separate cohorts defined by factors MFS and GROUP (patients/controls 1.5T, patients/controls 3T); routine 5—registration into two equal cohorts defined by random assignation of scans irrespective of diagnostic class or magnetic field strength; routine 6—registration to a "balanced" template created from equal numbers of images from each of the eight possible subgroups defined by gender, disease status and MFS

Group	MFS	ROU 1	ROU 2	ROU 3	ROU 4	ROU 5	ROU 6
Patients	1.5 T	1	1	1	1	Random	Balanced
Patients	3 T	1	1	2	2	Random	Balanced
Controls	1.5 T	1	2	1	3	Random	Balanced
Controls	3 T	1	2	2	4	Random	Balanced

factor MFS with two levels – 1.5T and 3T. Total intracranial volume, age and gender are included in the model to control for the effects of these variables. The different data acquisition centres ($n = 28$) are entered as separate regressors in the form of dummy variables. The thresholds for statistical significance are set to $P < 0.05$, after family-wise error (FWE) correction for multiple comparisons across the whole brain.

We compute and report the following *F*-tests for each of the six ROUTINES separately: main effects of factor MFS, main effect of GROUP, interaction analysis between these two factors. Additionally, in order to evaluate directly the impact of pre-processing ROUTINE on differentiation between AD patients and control subjects we conduct analyses using a flexible factorial design with factor GROUP (two levels) and factor ROUTINE (six levels). Given the fact that the design included repeated measurements from the same subjects for the factor routine, diagonal and non-zero off-diagonal parameters of the covariance matrix were estimated using restricted maximum likelihood—ReML (Friston et al. 2002).

RESULTS

Demographic and Clinical Data Analysis

The mean MMSE score in AD patients was 22.85 (range 20–26) and in control subjects – 29.25 (range 26–30). We report a significant main effect of the factor GROUP with significant ($P < 0.001$) lower MMSE scores in AD patients than healthy controls. There is no significant main effect for the factor MFS regarding MMSE score or age differences (MMSE $P > 0.475$; and age $P > 0.5$).

Voxel-based Morphometry Analysis

Main effect of factor

Magnetic field strength. *F*-tests are conducted separately for each registration strategy comparing data collected at 1.5 and 3 T, irrespective of the factor GROUP (Fig. 1). Data processed with ROUTINES 1, 2 and 5 reveals identical results regarding the MFS main effect. We report significant differences in the left ($x\ y\ z$: −6, −46, −29) and right ($x\ y\ z$: 11, −48, −30) cerebellum, left ($x\ y\ z$: −32, −19, 69) and right ($x\ y\ z$: 24, −19, 75) precentral gyri, left ($x\ y\ z$: −14, −24, 9) and right ($x\ y\ z$: 11, −27, 7) thalamus. For ROUTINES 3 and 4 we find additional MFS-related changes in the left frontal lobe ($x\ y\ z$: −18, 66, −18). ROUTINE 6 produced no significant results at a statistical threshold of $P < 0.05$ after FWE correction for multiple comparisons.

Main effect of factor GROUP. F-tests are conducted separately for each registration strategy irrespective of the factor MFS. We report identical findings for ROUTINES 1, 3, 5 and 6 consisting of grey matter volume decrease in the left ($x\ y\ z$: −23, −1, −20) and right ($x\ y\ z$: 29, 2, −20) hippocampus with lowest level of statistical significance for ROUTINE 6 (Figs. 2 and 3). For ROUTINE 2 and 4 we report additional significant differences in the left anterior middle temporal gyrus ($x\ y\ z$: −44, −6, −23) and the left caudate nucleus ($x\ y\ z$: −11, 11, 15).

Interaction between factors magnetic field strength and GROUP for each ROUTINE. There is no significant interaction between the factors MFS and GROUP for ROUTINE 1, 2, 3, 5 and 6. For ROUTINE 4 we find a significant effect in the cerebellum ($x\ y\ z$: 8, −46, −30; 11, −48, −30) and precentral gyri bilaterally ($x\ y\ z$: 29, −21, 72; 14, −24, 11), the left middle orbital gyrus ($x\ y\ z$: 8, 70, 14) and the right cuneus ($x\ y\ z$: 14, −72, 21).

Main effect of ROUTINE. We report a significant main effect of ROUTINE (irrespective of factors MFS and GROUP) with widespread changes across the whole brain and local maxima in the left middle temporal gyrus.

Interaction between factors magnetic field strength and GROUP irrespective of ROUTINE. There was no significant interaction between MFS and GROUP when analysis was conducted not controlling for ROUTINE.

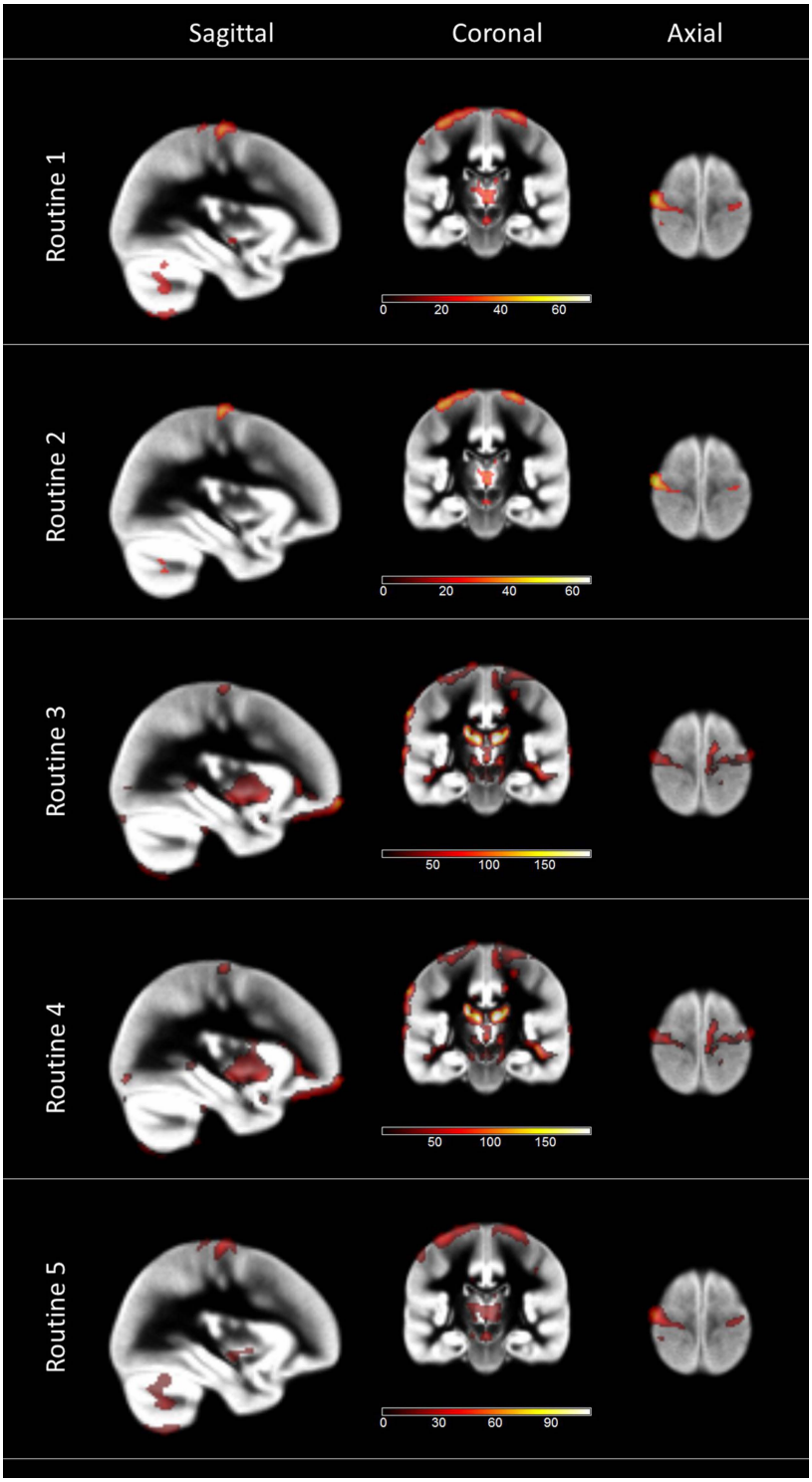

Figure 1.

Statistical parametric maps demonstrating the effect of magnetic field strength (MFS) at 1.5 Tesla vs. 3 Tesla on brain structure irrespective of GROUP and ROUTINE. SPM maps are thresholded at $P < 0.05$ FWE corrected, peak-level with colour bar indicating *F*-values. [Color figure can be viewed in the online issue, which is available at wileyonlinelibrary.com.]

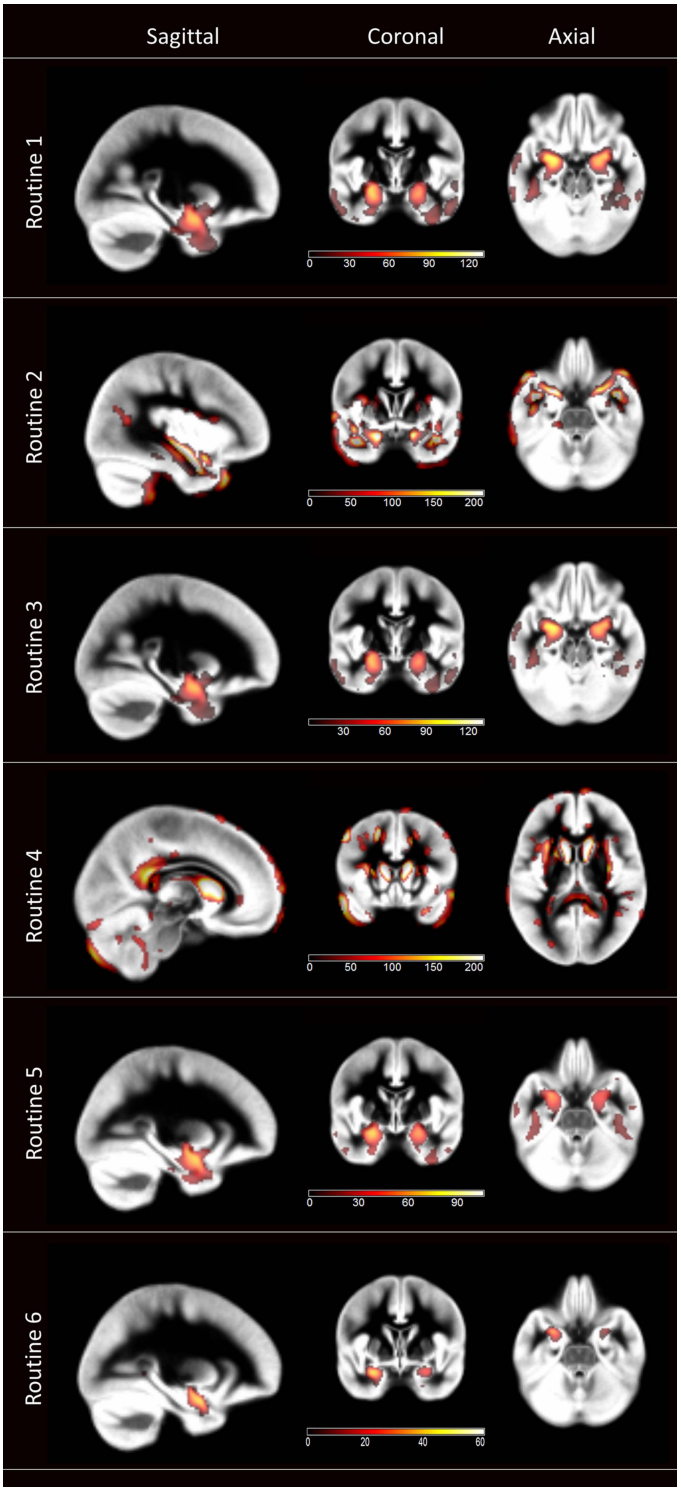

Figure 2.

Statistical parametric maps demonstrating the effect of GROUP – AD patients vs. healthy controls, irrespective of the pre-processing ROUTINE and MFS. SPM maps are thresholded at $P < 0.05$ FWE corrected, peak-level with colour bar indicating *F*-value. [Color figure can be viewed in the online issue, which is available at wileyonlinelibrary.com.]

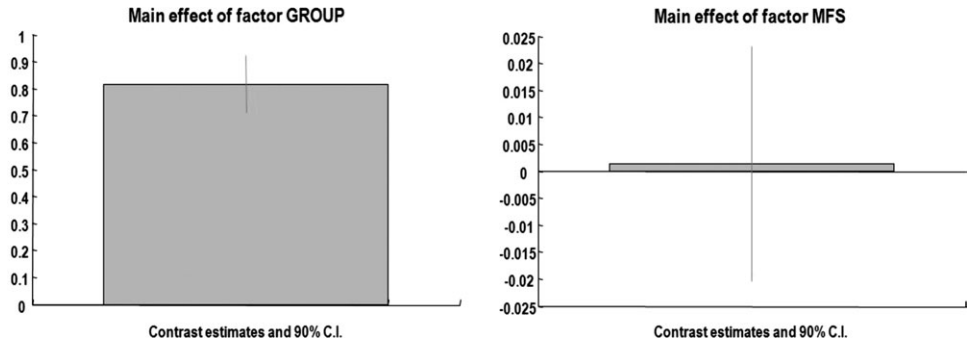

Figure 3.
Contrast estimates and 90% confidence intervals for main effect of the factors GROUP and MFS in the left media temporal lobe in ROUTINE 1.

Post-hoc Analyses

Based on the obtained results we conducted additional pair-wise analyses aiming at comparison between the most commonly applied registration strategies in single-centre studies (i.e. common and balanced study templates). We report a significant effect of factor ROUTINE irrespective of factors GROUP and MFS with widespread changes across the whole brain and local maxima in the left cerebellum and cingulate gyrus. There was no significant interaction between ROUTINE and GROUP.

DISCUSSION

Our study demonstrates significant effects of MFS and spatial registration strategy on brain anatomy when exploring multi-centre structural MR imaging data in patients with a neurodegenerative disorder—Alzheimer's disease. The obtained results, when tested for face validity based on pathological findings and previous computational anatomy studies in Alzheimer's disease lead us to conclude that for statistical group comparisons the optimal registration strategy for multi-site data collected at different MFS is provided by pooling all the image data irrespective of disease status or site of acquisition. To our knowledge this is the first empirical evidence for using a common registration strategy within a diffeomorphic algorithmic framework.

Magnetic Field Strength Effect

The study demonstrates grey matter volume differences related to MFS in cerebellum, precentral cortex and thalamus bilaterally. This is consistent with findings showing regional impacts of scanner type and field strength on VBM results and volume measurements of subcortical brain structures (Goodro et al., 2012; Pardoe et al., 2008; Pfefferbaum et al., 2012; Stonnington et al., 2008; Tardif et al., 2010). One possible interpretation of the differential estimation of regional volumes includes dependency of the segmentation procedure on brain tissue properties detected at specific field strengths. It has been shown that in areas where segmentation of tissue classes is usually difficult due to low grey-white matter contrast and/or complex patterns of cortical folding, the accuracy of segmentation improves at 3T. Our findings are consistent with previously reported effect of MFS effects on brain volume estimation, particularly in motor cortex and cerebellum (Tardif et al., 2010). On the other hand, it is also possible that the high content of intracortical myelin in the precentral gyrus in addition to paramagnetic iron within the cerebellar nuclei could produce differences in MR contrast at different MFS and subsequently in tissue classification (Deoni and Catani, 2007). This interpretation is supported by the fact that T1, T2 and T2* relaxivity are increased due to differential ferromagnetic properties of iron, thus causing greater signal alteration of iron-laden tissue with increasing MFS.

The changes we report in the thalamus may be interpreted as specific features related to the ADNI MPRAGE protocol. The assumption here is that the grey/white matter contrast-to-noise ratio improves at 3T especially for subcortical structures, however it is considerably lower than the grey/white matter contrast in cortex. This is a consequence of differential T1 relaxation times for subcortical and cortical grey matter modulated further by the local B1 field. As a result, contrast non-uniformity at 3T can shift the tissue boundaries and lower the accuracy of grey matter classification of deep brain structures such as the thalamus (Scorzin et al., 2008; Tardif et al., 2010). The observed thalamic differences at 3T and 1.5T in earlier studies are interpreted more generally as a reflection of dielectric variance at different MFSs, manifesting as signal inhomogeneities in the centre of the brain at 3T compared to 1.5T (Pardoe et al., 2008; Tanenbaum, 2006).

We confirm that the effect of magnetic field on the computational assessment of brain anatomy is substantially smaller than that of disease, and that there is no interaction between MFS and the presence of AD. Both results

justify pooling data from different scanners of variable MFS—a conclusion that may be even more useful to those studying rare diseases than for studies of more common neurodegenerative disorders. There may still be a need for further similar, disease-specific studies where different patterns of structural change are expected. For example, it may be that the almost negligible effect of MFS in the hippocampal areas in our study is attributable to the high quality of the data collected by ADNI (Jack et al., 2008). The ADNI acquisition protocol was optimized to provide high quality data (including signal-to-noise-ratio) on all hardware platforms. It is also possible that scanning parameters interact with MFS thus modulating VBM comparisons, which is the case in pre-motor areas, or resulting in differential performance of the bias field correction. A recent study has shown that inconsistency in voxel size may influence VBM results (Pereira et al., 2008). An alternative approach for controlling the effects of MFS and potential interactions is to model them directly in the design matrix.

Influence of Image Registration Strategy

We investigated how the user-dependent choice of different image registration strategies for data acquired at multiple sites influences VBM results in Alzheimer's disease. We demonstrate that a spatial registration strategy of pooling all data disregarding disease status or scanner (study site and/or MFS) produces results with the greatest validity in terms of biological plausibility (Frisoni et al., 2010). The analyses using various combinations of cohorts to estimate disease/site-specific registration parameters fail to provide the same level of performance and at times introduce artefacts especially at the edges of grey matter maps. We report the same spatial pattern of differences between groups when images are registered within subcohorts specified by the magnetic field (irrespective of diagnosis), randomly divided in two subgroups and registered to the balanced study template. However, the lowest statistical power was found for random and balanced templates, which shows that DARTEL-based registration works optimally when applied to all the images in a study cohort. Additional post-hoc analyses show no significant interaction between selected registration strategies (most frequently in single-centre studies – i.e. common and balanced study templates) with the disease status. One possible explanation for the lower statistical power of our structural findings when using registration based on a balanced template could be related to the fact that some subgroups were not well represented – only 7 out of 22 male patients scanned at 3T were included in the balanced template.

The remaining strategies, which averaged and selected features to be conserved separately for control and AD subjects or MFSs, resulted in biologically implausible regional patterns of structural changes. We interpret this result as an effect of bias in image registration caused by segregating study cohorts. This conclusion and result are consistent with the demonstration that systematic shape differences between cohorts can strongly influence VBM comparisons. Specifically, this effect was first reported by Gitelman et al. (2001) in the caudate nucleus and explained as a consequence of group differences in ventricular size.

Our results are consistent with this interpretation considering the fact that ventricular enlargement is an objective and sensitive measure of neuropathological change associated with neurodegenerative disease (Nestor et al., 2008). The same logic applies to a regional effect in the anterior middle temporal gyrus with enlargement of the hippocampal sulcus in AD patients, which is likely to result in registration ambiguity caused by systematic group shape differences (Bastos-Leite et al., 2006). To our knowledge this issue, related to creation of disease/group-specific templates in the DARTEL framework is still an open question. Our results show empirically how the choice of registration strategy influences VBM results. However, though cohort-specific templates interfere with accurate spatial registration and might lead to a higher number of false positives (Hua et al., 2008) it remains likely that they contribute potential additional information about cohort-specific anatomy (Mandal et al., 2012).

Limitations

There are several potential technical limitations of our study having implication on the validity of registration strategy recommendation. Here, we analysed only one of the most frequent measures used in brain imaging studies that is grey matter volumes derived from T1w images. Further studies of different tissue types and image sequences are needed to confirm and generalise the results we report here. In addition, we used SPM8 software and the DARTEL diffeomorphic registration approach, which also might limit the generalisability of the observed effects to other open source software available to the neuroimaging community. It is also worth to mention that for the case of large multi-site studies the creation of the recommended common anatomical template pooling all available data could become a burden due to the fact that the diffeomorphic registration step in SPM is computationally time consuming. Finally, further studies on pre-clinical disease states and comparisons of different types of dementia, such as FTD vs. AD are needed.

CONCLUSION

Our work is motivated by a rapidly growing tendency for sharing, pooling and testing data in multi-centre MRI studies of neurodegeneration (Di Perri et al., 2009; Lotjonen et al., 2011; Stonnington et al., 2008). Our findings clearly indicate that when using diffeomorphic registration

algorithms for multi-centre MRI studies the optimal registration strategy is to pool all study images to create a common anatomical template irrespective of disease status, or MFS.

ACKNOWLEDGMENTS

This work was financially supported by Scientific Exchange Programme NMS-CH grant.

BD is supported by the Swiss National Science Foundation (grant Nr 320030_135679 and NCCR Synapsy), Foundation Parkinson Switzerland, Foundation Synapsis, Novartis Foundation for medical–biological research and Deutsche Forschungsgemeinschaft (Kfo 247). FK is supported by the Velux Stiftung, Switzerland.

The funders had no role in study design, data collection and analysis, decision to publish, or preparation of the manuscript.

REFERENCES

Ashburner J, Friston KJ (2000): Voxel-based morphometry – The methods. NeuroImage 11:805–821.

Ashburner J, Friston KJ (2005): Unified segmentation. NeuroImage 26:839–851.

Ashburner J (2007): A fast diffeomorphic image registration algorithm. Neuroimage 38:95–113.

Bastos-Leite AJ, van Waesberghe JH, Oen AL, van der Flier WM, Scheltens P, Barkhof F (2006): Hippocampal sulcus width and cavities: Comparison between patients with Alzheimer disease and nondemented elderly subjects. AJNR Am J Neuroradiol 27:2141–2145.

Braak H, Braak E (1991): Neuropathological stageing of Alzheimer-related changes. Acta Neuropathol 82(4):239–259.

Briellmann RS, Syngeniotis A, Jackson GD (2001): Comparison of hippocampal volumetry at 1.5 Tesla and 3 Tesla. Epilepsia 42:1021–1024.

Deoni SCL, Catani M (2007): Visualization of the deep cerebellar nuclei using quantitative T1 and rho magnetic resonance imaging at 3 Tesla. NeuroImage 37:1260–1266.

Dickerson BC, Fenstermacher E, Salat DH, Wolk DA, Maguire RP, Desikan R, Pacheco J, Quinn BT, Van der Kouwe A, Greve DN, Blacker D, Albert M, Killiany RJ, Fischl B (2008): Detection of cortical thickness correlates of cognitive performance: Reliability across MRI scan sessions, scanners, and field strengths. NeuroImage 39:10–18.

Di Perri C, Dwyer MG, Wack DS, Cox JL, Hashmi K, Saluste E, Hussein S, Schirda C, Stosic M, Durfee J, Poloni GU, Nayyar N, Bergamaschi R, Zivadinov R (2009): Signal abnormalities on 1.5 and 3 Tesla brain MRI in multiple sclerosis patients and healthy controls. A morphological and spatial quantitative comparison study. Neuroimage 47:1352–1362.

Focke NK, Helms G, Kaspar S, Diederich C, Tóth V, Dechent P, Mohr A, Paulus W (2011): Multi-site voxel-based morphometry – Not quite there yet. Neuroimage 56(3):1164–1170.

Frisoni GB, Fox NC, Jack CR, Scheltens P, Thompson PM (2010): The clinical use of structural MRI in Alzheimer disease. Nat Rev Neurol 6:67–77.

Friston K, Penny W, Phillips C, Kiebel S, Hinton G, Ashburner J (2002): Classical and Bayesian inference in neuroimaging: Theory. NeuroImage 16:465–483.

Gitelman DR., Ashburner J, Friston KJ, Tyler LK, Price CJ (2001): Voxel-based morphometry of herpes simplex encephalitis. NeuroImage 13:623–631.

Goodro M, Sameti M, Patenuade B, Fein G (2012): Age effect on subcortical structures in healthy adults. Psychiatry Res. Neuroimaging 203(1):38–45.

Han X, Jovicich J, Salat D, Van der Kouwe A, Quinn B, Czanner S, Busa E, Pacheco J, Albert M, Killiany P, Maguire P, Rosas D, Makris N, Dale A, Dickerson B, Fischl B (2006): Reliability of MRI-derived measurements of human cerebral cortical thickness: The effects of field strength, scanner upgrade and manufacturer. NeuroImage 32:180–194.

Hua X, Leow AD, Lee S, Klunder AD, Toga AW, Lepore N, Chou YY, Brun C, Chiang MC, Barysheva M, Jack CR Jr, Bernstein MA, Britson PJ, Ward CP, Whitwell JL, Borowski B, Fleisher AS, Fox NC, Boyes RG, Barnes J, Harvey D, Kornak J, Schuff N, Boreta L, Alexander GE, Weiner MW, Thompson PM, Alzheimer's Disease Neuroimaging Initiative (2008): 3D characterization of brain atrophy in Alzheimer's disease and mild cognitive impairment using tensor-based morphometry. Neuroimage 41:19–34.

Hyman BT (1997): The neuropathological diagnosis of Alzheimer's disease: Clinical–pathological studies. Neurobiol Aging 18:S27–S32

Jack CR Jr., Bernstein MA, Fox C, Thompson PM, Alexander G, Harvey D, Borowski B, Britson PJ, Whitwell J, Ward C, Dale AM, Felmlee JP, Gunter JL, Hill DL, Killiany R, Schuff N, Fox-Baosetti S, Lin C, Studholme C, DeCarli CS, Krueger G, Ward HA, Metzger GJ, Scott KT, Mallozzi R, Blezek D, Levy J, Debbins JP, Fleisher AS, Albert M, Green P, Bartzokis G, Glover G, Mugler J, Weiner MW (2008): The Alzheimer's Disease Neuroimaging Initiative (ADNI): MRI methods. J Magn Reson Imag 27:685–691.

Klein A, Andersson J, Ardekani BA, Ashburner J, Avants B, Chiang M-C, Christensen GE, Collins DL, Gee J, Hellier P, Song JH, Jenkinson M, Lepage C, Rueckert D, Thompson P, Vercauteren T, Woods RP, Mann JJ, Parsey RV Christensen GE, Collins DL, Gee J, Hellier P, Song JH, Jenkinson M, Lepage C, Rueckert D, Thompson P, Vercauteren T, Woods RP, Mann JJ, Parsey RV (2009): Evaluation of 15 nonlinear deformation algorithms applied to human brain MRI registration. NeuroImage 46:786–802.

Lepore N, Brun C, Yi-Yu Chou, Lee AD, Barysheva M, Pennec X, McMahon KL, Meredith M, de Zubicaray GI, Wright MJ, Toga AW, Thompson PM (2008): Best individual template selection from deformation tensor minimization Proceedings of the 5th IEEE International Symposium on Biomedical Imaging (ISBI), Paris, France, May 14–17.

Lotjonen J, Wolz R, Koikkalainen J, Julkunen V, Thurfjell L, Lundqvist R, Waldemar G, Soininen H, Rueckert D, Alzheimer's Disease Neuroimaging Initiative (2011): Fast and robust extraction of hippocampus from MR images for diagnostics of Alzheimer's disease. NeuroImage 56:185–196.

Mandal PK, Mahajan R, Dinov ID. Structural Brain Atlases: Design, rationale, and applications in normal and pathological cohorts (2012). J Alzheimers Dis 31(0):S169–S188.

Mueller SG, Weiner MW, Thal LJ, Petersen, RC, Jack C, Jagust W, Trojanowski, JQ, Toga AW, Beckett L (2005): The Alzheimer's

Disease Neuroimaging Initiative. Neuroimaging Clin N Am 15:869–877.

Nestor SM, Rupsingh R, Borrie M, Smith M, Accomazzi V, Wells JL, Fogarty J, Bartha R (2008): Alzheimer's Disease Neuroimaging Initiative ventricular enlargement as a possible measure of Alzheimer's disease progression validated using the Alzheimer's Disease Neuroimaging Initiative database. Brain 131:2443–2454.

Pardoe H, Pell GS, Abbott DF, Berg AT, Jackson GD (2008): Multi-site voxel-based morphometry: Methods and a feasibility demonstration with childhood absence epilepsy. NeuroImage 42:611–666.

Pereira JM, Nestor PJ, Williams GB (2008): Impact of inconsistent resolution on VBM studies. Neuroimage 40:1711–1717.

Pereira JMS, Xiong L, Acosta-Cabronero J, Pengas G, Williams GB, Nestor PJ (2010): Registration accuracy for VBM studies varies according to region and degenerative disease grouping. NeuroImage 49:2205–2215.

Pfefferbaum A, Rohlfing T, Rosenbloom MJ, Sullivan EV (2012): Combining atlas-based parcellation of regional brain data acquired across scanners at 1.5 T and 3.0 T field strengths Neuroimage 60:940–951.

Raz, N, Lindenberger U, Rodrigue KM, Kennedy KM, Head D, Williamson A, Dahle C, Gerstorf D, Acker JD (2005): Regional brain changes in aging healthy adults: General trends, individual differences and modifiers. Cereb Cortex 15:1676–1689.

Scorzin JE, Kaaden S, Quesada CM, Muller CA, Fimmers R, Urbach H, Schramm J (2008): Volume determination of amygdala and hippocampus at 1.5 and 3.0 T MRI in temporal lobe epilepsy. Epilepsy Res 82:29–37.

Stonnington CM, Tan G, Klöppel S, Chu C, Draganski B, Jack CR Jr, Chen K, Ashburner J, Frackowiak RS (2008): Interpreting scan data acquired from multiple scanners: A study with Alzheimer's disease. Neuroimage 39:1180–1185.

Takahashia R, Ishiice K, Miyamotoc N, Yoshikawac T, Shimadad K, Ohkawa S, Kakigi T, Yokoyama K (2010): Measurement of grey and white matter atrophy in dementia with Lewy bodies using diffeomorphic anatomic registration through exponentiated Lie Algebra: A Comparison with conventional voxel-based morphometry. AJNR Am J Neuroradiol 31:1873–1878.

Tanenbaum LN (2006): Clinical 3T MR imaging: Mastering the challenges. Magn Reson Imag Clin N Am 14:1–15.

Tardif CL, Collins DL, Pike GB (2010): Regional impact of field strength on voxel-based morphometry results. Hum Brain Mapp 31:943–957.